This article has been accepted for publication in a future issue of this journal, but has not been fully edited. Content may change prior to final publication. Citation information: DOI 10.1109/TBME.2018.2865751, IEEE Transactions on Biomedical Engineering

Noninvasive Cuffless Blood Pressure Estimation Using Pulse Transit Time and Impedance Plethysmography

Toan Huu Huynh, Roozbeh Jafari, *Senior Member, IEEE* and Wan-Young Chung*, *Senior Member, IEEE*

***Abstract*—*Objective:* To demonstrate the feasibility of everaging impedance plethysmography (IPG) for detection of pulse transit time (PTT) and estimation of blood pressure (BP). *Methods:* We first established the relationship between BP, PTT, and arterial impedance (i.e., the output of IPG). The IPG sensor was placed on the wrist while the photoplethysmography (PPG) sensor was attached to the index finger to measure the PTT. With a cuff-based BP monitoring system placed on the upper arm as a reference, our proposed methodology was evaluated on 15 young, healthy human subjects with handgrip exercises as interventions and compared to several conventional PTT models to assess the efficacy. *Results:* The proposed model correlated with BP fairly well with group average correlation coefficients of 0.88 ± 0.07 for systolic BP (SBP) and 0.88 ± 0.06 for diastolic BP (DBP). In comparison with the other PTT methods, PTT-IPG-based BP estimation achieved a lower root-mean-squared-error (RMSE) of 8.47 ± 0.91 mmHg and 5.02 ± 0.73 mmHg for SBP and DBP, respectively. *Conclusion:* We conclude that the measurement of arterial impedance via IPG methods is an adequate indicator to estimate BP. The proposed method appears to offer superiority compared to the conventional PTT estimation approaches. *Significance:* Using impedance magnitude to estimate PTT offers promise to realize wearable and cuffless BP devices.**

***Index Terms*—Cuffless blood pressure, pulse transit time (PTT), impedance plethysmography (IPG), radial impedance.**

I. Introduction

BLOOD pressure (BP) monitoring is of significant importance to control and prevent hypertension, especially for the elderly. Due to the impact of this disorder on a large number of individuals, 1 billion worldwide, many researchers have attempted to improve the methods of BP measurement. There are several noninvasive BP methods. Auscultation is the standard clinical method, whereas oscillometry is the most popular automatic method for ambulatory BP monitoring. Because of the bulky and manual nature of these systems, the volume-clamp method has been proposed. This method measures finger arterial pressure using a cuff in combination with a photoplethysmography (PPG) sensor. Although this system is more convenient, using a finger cuff still presents a drawback for long-term BP monitoring. Without requiring an inflatable cuff, the tonometry method measures radial artery BP by pressing an array of pressure sensors against the skin. Even though few automatic tonometry devices have been developed, a high sensitivity to the positioning of the force sensor remains as a principal disadvantage. There are still other existing BP monitoring methods however none is suitable for ubiquitous BP monitoring [1].

One proposed method that addresses the above challenges relies on measurement of pulse transit time (PTT), which is the time interval of the pulse wave propagation between two arterial sites and is affected by BP [1, 2]. The PTT is inversely proportional to the BP. High BP corresponds to high pulse wave velocity (PWV) which in turn means a low PTT value. The Moens-Korteweg equation shows the relationship between PWV and elastic modulus E through the following expression:

$$PWV = \frac{D}{PTT} = \sqrt{\frac{Eh}{\rho d}} \quad (1)$$

PWV can be obtained by the ratio of the distance D between the two arterial sites and PTT. With ρ as density of blood, h as the wall thickness and d as the diameter of the artery, the assumption is that E alone is a variable related to BP; therefore, PTT can be converted to BP values with an initial calibration.

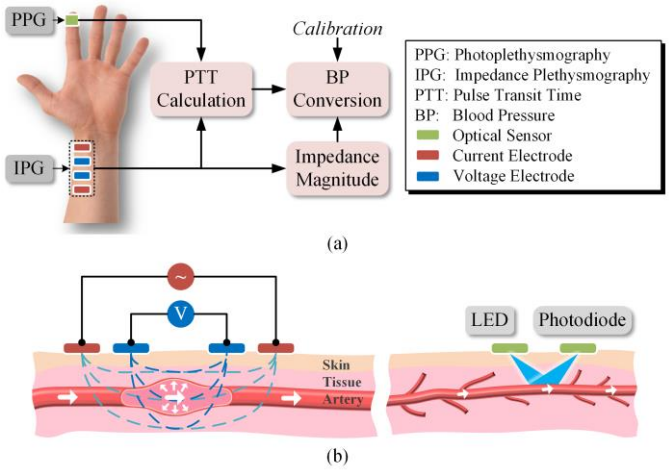

Fig. 1. Overview of the methodology used in this study. (a) Block diagram of the proposed PTT-IPG-based BP model. (b) Overview of experimental setup with IPG sensor at radial artery and PPG sensor at digital artery.

This work (2016R1A2B4015) was supported by Mid-Career Researcher Program through an NRF grant funded by MEST, Korea.

Toan Huu Huynh is with Department of Electronic Engineering, Pukyong National University, Busan 608-737, South Korea (e-mail: tanhinh@pukyong.ac.kr).

Many investigations have shown that the PTT-based methods provide a good estimate for BP [1-5].

Although PTT-based methods are promising, there are still some challenges that need to be addressed before their widespread application. Firstly, experimental results show that the elastic modulus *E* depends not only on BP but also the age of central arteries [6], while BP and smooth muscle (SM) mainly affect the peripheral elasticity [7]. Therefore, reliance on the relationship between *E* and BP alone impacts PTT-based BP estimation accuracy. The second challenge of the PTT method is the independent determination of systolic and diastolic BP, referred to as SBP and DBP, respectively. A single PTT value has been used to access two BP levels, meaning one of those values may be inaccurate. Only SBP is estimated in some studies [8, 9], while some PTT-BP models could obtain just DBP [10, 11] or mean blood pressure (MBP) [10, 12]. To address this problem, a few studies consider a variety of PTT determination [13-15]. Last but not least, if the pulse waveforms cannot be easily detected, the PTT method is obviously will not produce suitable outcome. The typical PTT model utilizes electrocardiography (ECG) as the proximal waveform and photoplethysmography (PPG) as the distal timing reference. The biggest advantage of the ECG method is the high reliability of the R-wave which is easy to detect and less sensitive to motion artifacts. However, ECG electrodes are often required to be affixed to the chest, hands, and legs, which is inconvenient for the patients [16]. Moreover, using the ECG waveform yields the pulse arrival time (PAT) instead of PTT. PAT is the sum of PTT and the pre-ejection period (PEP) [1]. Since PEP is uncorrelated to BP, several studies use PPG or impedance cardiography (ICG) instead of ECG to eliminate the PEP value [14, 17]. Some PTT-based BP estimations using two or multiple PPG sensors in the peripheral arteries have improved the user comfort [18-20]. However, the accuracy of these systems still needs improvements [1, 11, 18]. Holz and Wang designed glasses prototype using optical sensors and inertial sensors to extract PTT values [21]. However, the sensor attachment on glasses may cause inaccurate recordings. Moreover, glasses may not be convenient for users who do not suffer from eye disease. Recently, a SeismoWatch has been introduced using seismocardiogram (SCG) and PPG sensors [22]. Unfortunately, this approach cannot be applied for continuous BP monitoring since the user must hold the device against the sternum to detect micro-vibrations of the chest wall.

Apart from the PTT, arterial cross-sectional area has been shown to be a reliable marker of BP. The change in BP is directly proportional to the change in arterial cross-sectional area. Unlike PTT, the arterial diameter is continuously affected by BP during the whole cycle of cardiac activity, thereby impacting both SBP and DBP [23, 24]. Using arterial cross-sectional area or diameter parameters may solve the independent determination of SBP and DBP which is derived by a single PTT measurement. Moreover, with these indicators, PTT-based BP estimation can offer higher accuracy since the elastic modulus *E* is dependent on both the BP and arterial radius [25], as shown below:

$$E = \frac{\Delta P}{\Delta R}\frac{2(1-\sigma^2)R_0R_i^2}{R_0^2 - R_i^2} \tag{2}$$

where the ΔR is the change in the external radius following a pressure change ΔP, R_i is the internal radius, R_0 is the external radius, and σ is known as Poisson's ratio.

Both the PPG and impedance plethysmography (IPG) techniques have been widely used to detect changes in the blood volume, thus mainly reflecting changes in arterial volume and dimension. Whereas the PPG sensor must fit tightly onto the body surface in the perpendicular direction, the IPG sensor only needs to contact slightly to the skin to produce electric potential fields. Compared to strong PPG contact to the skin, the electrodes of IPG method could be made from the soft and flexible material that could bring some benefits for the users. In addition, PPG method requires a light-emitting source and a photodetector that may need to consume much power. Moreover, the IPG system is less sensitive to the measured location than PPG. With these notable aspects of arterial cross-sectional area measurement in mind, to improve the BP measurement accuracy, this paper proposes to employ PTT measurement in conjunction with IPG. IPG is a noninvasive method for measuring the arterial impedance *Z* of peripheral arteries, which is directly affected by the arterial cross-sectional area *A* as follows.

$$A = \rho L / Z \tag{3}$$

where *L* represents the length of the measured segment. Using the IPG waveform as the proximal timing reference can produce a PTT value instead of PAT and is more conveniently detected in comparison with ECG method. As shown in Fig. 1, the proposed measurements are performed with the IPG sensor at the wrist on the radial artery, and the PPG sensor on the index finger, thus constituting a new wearable BP device offering ubiquitous monitoring.

II. Materials and Methods

A PTT-IPG model has been studied to show the relationship between PTT, radial impedance, and BP. A measurement system is also developed to apply in the proposed BP model. For further evaluation, this study designs a validation protocol leveraging a gold standard reference device.

A. Blood Pressure Estimation

The arterial vessel is often modeled as an elastic cylindrical tube. The compliance *C* of the tube has shown to be related to the geometry of the arterial vessel and the elastic modulus of the arterial wall. In other words, the compliance *C* is characterized in terms of the changes in cross-sectional area *A* and pressure *P* (i.e., *dA/dP*) [23].

The propagation velocity, which represents vasculature elasticity, is inversely related to the compliance *C*. According to the Bramwell-Hill equation, PWV is determined by the compliance *C* with ρ/A representing the arterial inertance per unit length.

$$PWV = \sqrt{\frac{AdP}{\rho dA}} \tag{4}$$

Taking Equation (4) a step further and integrating *dP* and *dA*, the pressure can be written in terms of PWV and the cross-sectional area A as follows.

$$P(t) = P_0 + \rho PWV^2 \ln\left(\frac{A(t)}{A_0}\right) \quad (5)$$

where P_0 is the pressure corresponding to the cross-sectional area A_0 [26]. The total segment is regarded as the parallel model of the blood and tissue. With Z_a and Z_t as the impedance of the artery and tissue respectively, the impedance of a body segment Z derived from IPG measurement is given by [27]:

$$1/Z = 1/Z_a + 1/Z_t \quad (6)$$

Since the tissue impedance is assumed to remain constant, from Equations (3) and (6), the change in arterial cross-sectional area ΔA can be expressed as a function of the change in measured impedance ΔZ.

$$\Delta A \approx \rho_b L \Delta Z / Z_b^2 \quad (7)$$

in which ρ_b is the resistivity of blood and Z_b represents the basal impedance of the segment. The cross-sectional area over time is given by the sum of the original A_0 and the change ΔA of cross-sectional area; therefore, BP can be expressed in term of PTT and the impedance Z of body segment. By replacing PWV with a function of PTT and taking Equation (5) some simple steps further using (7), the BP values can be obtained as follows:

$$P(t) = P_0 + \rho \frac{D^2}{PTT^2} \ln\left[1 + K\left(Z_0 - Z(t)\right)\right] \quad (8)$$

where K is a constant and is equal to Z_{a0}/Z_0^2. At the pressure P_0, Z_{a0} represents the arterial impedance and Z_0 is the impedance of the body segment while P(t) can be replaced by SBP or DBP. In each cardiac cycle, the PTT value has been used for both SBP and DBP, while the highest and lowest points of the impedance waveform are separately employed for the two BP levels. Impedance Z is inversely related to BP through the cross-sectional area, thus, Z_{min} is utilized to estimate SBP while DBP can be obtained through Z_{max}.

An initial calibration is done to determine the calibrated parameters including a pair of measurements from the BP reference device and the proposed device. Based on the influence of BP to impedance Z, the original parameters in Equation (8) can be determined corresponding to the calibrated DBP level (P_0). The calibrated SBP value (in terms of P(t)) and two impedance values (in terms of Z_0 and Z(t)) are used to calculate the subject-specific K. Thereupon, with the constant distance D calculated from the wrist to the finger and the measured PTT, beat-to-beat BP can be estimated.

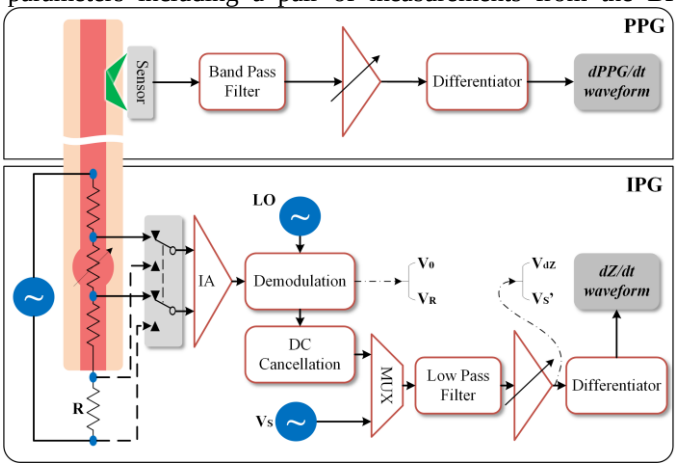

Fig. 2. The designed system for detecting IPG and PPG waveforms. The dash-dotted lines represent the output parameters. In a set of two parameters, only one output is measured corresponding to different inputs of the multiplexer.

B. Measurement System

1) System Design

As described in Fig. 2, the complete system includes two parts. The first component is impedance measurement with the IPG sensor located on the radial artery at the wrist. The second component, the PPG system, is placed at the index finger for pulse waveform detection.

The IPG hardware is designed based on a tetrapolar configuration to provide enhanced accuracy for detection of both the magnitude and the phase of the impedance waveform. Current injection and voltage detection are performed using two pairs of electrodes. The radial impedance is obtained through the measured voltage and injected current according to the Ohm's law [27]. This study uses 500 μA at 100 kHz for the current source because these parameters are safe for the human body and can sufficiently assist with the detection of the impedance variations [28]. In addition, flexible dry-contact electrodes are employed to improve user comfort and allow long-term monitoring. Conductive electrodes made of silver-plated polyester could be soft, bendable, and stretched in both directions. The electrode-skin impedance is 133 Ω @ 100 kHz with a thickness of 0.45 mm and a surface resistivity lower than 1 Ω/sq [29].

The Wien-bridge oscillator is implemented to generate high-frequency sine waves while a monopolar improved Howland current pump is utilized to realize a high-impedance constant current source. The small variation of the radial blood vessel is amplified using high-speed, low-noise instrumentation amplifier AD8421 with a high common-mode rejection ratio of 110 dB and a gain of 60 dB at 100 kHz. The gain is adjusted to realize a clear and unsaturated waveform. Using an accurate synchronous demodulation with AD630, the carrier signal and the interfering noise are removed and then, the basal impedance Zb is obtained. Next, the DC cancellation is applied, thereby allowing enhanced observation of the variation of measured impedance. Since the magnitude waveform after this stage is only a few millivolts, the next amplifier stage with the gain of 50 dB is required. An active 6th order low pass filter with the corner frequency at 3 Hz is used to remove noise and other undesirable frequency components. Finally, the impedance waveform is monitored with a programmable-gain amplifier. Also, this waveform is passed through a differential amplifier to acquire the dZ/dt waveform.

This article has been accepted for publication in a future issue of this journal, but has not been fully edited. Content may change prior to final publication. Citation information: DOI 10.1109/TBME.2018.2865751, IEEE Transactions on Biomedical Engineering

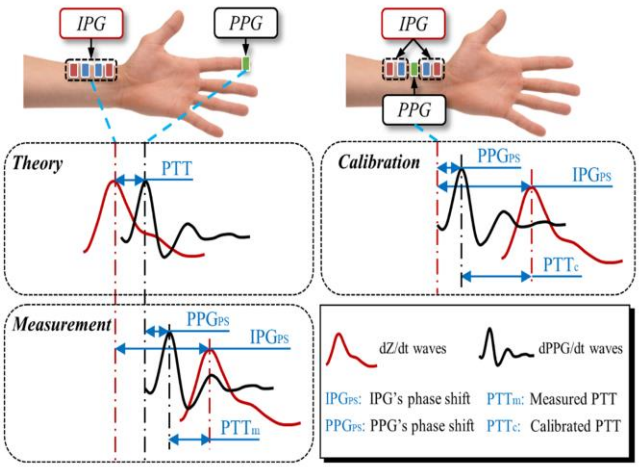

Fig. 3. Experimental PTT measurement and PTT calibration with both IPG and PPG sensors located at the same position at the wrist.

For PPG waveform detection, a reflected optical sensor RP320 (Laxtha, South Korea) has been employed. The first stage of this part is the active 4th order band pass filter to suppress the large DC component and also boost the small variations caused by the pulsatile blood volume. The upper and lower -3dB cut-off frequencies of this stage are 2.34 and 0.7 Hz, respectively with a gain of 40 dB. This stage also removes the unexpected DC signal and interference noise. To get a clear PPG waveform, a non-inverting amplifier with programmable gain is applied. Finally, a differentiator stage is used to obtain the *dPPG/dt* waveform.

The proposed system consumes 92 mW (28mA @3.3V) in practice, meeting the characteristics of a wearable device [30].

2) Parameter Determination

The total radial impedance is equal to the sum of the basal impedance Z_b and the impedance variation dZ. The voltage drop V_{Rcal} over the known resistor R of 100 Ohm is used to calibrate the base value Z_b. To calculate the actual impedance variation due to the changing blood volume, a small sine-wave V_S of 10 mV at 1 Hz is generated to obtain the gain of the amplifier chain. Multiplexer stages are implemented to switch between the calibrated and actual parameters. Finally, due to the linear influence, the real radial impedance can be computed as follows:

$$Z = Z_b + dZ = \frac{R}{V_R}\left(V_o + \frac{V_S}{V_S'}V_{dZ}\right) \tag{9}$$

By substituting Equation (9) for BP estimation in Equation (8), the expression $K(Z_0\text{-}Z)$ can be rewritten as $k(V_{dZ0}\text{-}V_{dZ})$ where k is a constant and equal to $K(R/V_R)(V_S/V_S')$. With an initial device-specific calibration, the measured voltage of the impedance waveform V_{dZ} can be leveraged to estimate BP values.

For PTT calculation, different time intervals between IPG and PPG waveforms are computed. Several studies employ peak-to-peak or foot-to-foot PTT determination [1, 13, 14], however, a single PTT may best correspond to one BP value. To address this challenge, as in some investigations [15, 31, 32], PTT is determined as the period between the peaks of first derivative of PPG and IPG waveform in each corresponding cardiac cycle.

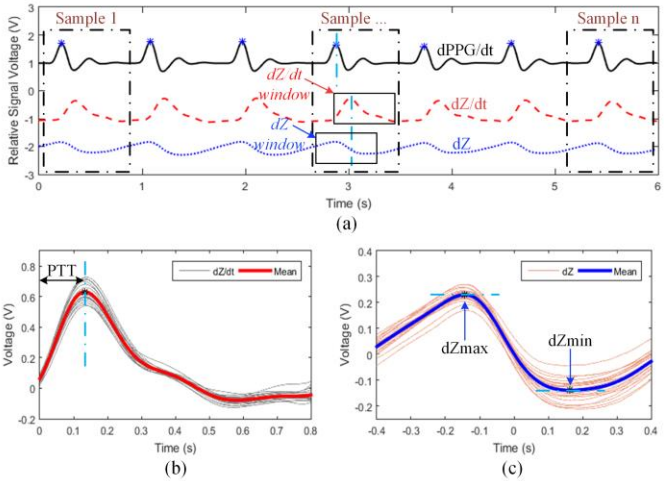

Fig. 4. (a) Representative all measured waveforms with the definition of collecting data frames. (b), (c) PTT and arterial impedance calculation using ensemble average with the peak of *dPPG/dt* and *dZ/dt* as the origin, respectively.

Due to the fact that the two separate pulse detection methods have a different phase shift, the actual PTT value varies significantly since the distance between the wrist and the finger is quite small. In addition to the PTT, the phase-difference time between sensors also need to be considered. Therefore, after eliminating or calibrating the time difference between different sensors, the remained time difference is caused by the pulse transit. The experimental results have shown that the PPG waveform lead the IPG waveform instead of lagging since the phase shift of IPG system is greater than the phase shift of PPG system and the desired PTT. Hence, PTT calibration is required. As shown in Fig. 3, the calibrated time delay is measured with both IPG and PPG sensors located at the same position on the wrist. The bracelet line was used as the origin for repeatable measurements. To control the pressure of the sensor on the skin, the DC output voltage was obtained from a pressure sensor shift after skin attachment. From the PTT measurement and calibration, the phase shift of IPG system can be expressed as follows:

$$IPG_{PS} = PTT + PPG_{PS} + PTT_m \tag{10a}$$

$$= PPG_{PS} + PTT_c \tag{10b}$$

By subtracting Equation (10a) from Equation (10b), the desired PTT can be written in term of the measured PTT and the calibrated PTT. The average of the calibrated PTT of the proposed system is around 0.15 seconds while the measured PTT varies with human subjects. After calibration, the negative or out-of-range PTT values (according to normal PWV range from 3 m/s to 15 m/s) are removed.

$$PTT = PTT_c - PTT_m \tag{11}$$

Furthermore, to prevent motion artifacts and acquire more reliable data, ensemble averaging has been applied. Unlike the IPG waveform, the *dPPG/dt* waveform is used only for pulse detection. Therefore, the corresponding time of the peak for that waveform is utilized as the reference time for each pulse beat. The ensemble frame is determined as the minimum cardiac

period. Finally, the average of this ensemble of all individual beats within 20 seconds has been used to calculate the PTT value and radial impedance magnitude as illustrated in Fig. 4.

C. Experimental Details

The experiments were performed on 15 healthy adults without any history of cardiovascular diseases such as hypertension (age: 29 ± 5 years; gender: 10 males, 5 females; height: 164 ± 8 cm; weight: 60 ± 9 kg). The ambulatory BP monitoring Oscar 2 system (SunTech Medical, USA) which passed three internationally recognized standards has been used as the reference. The proposed system was located at the wrist (IPG sensor) and the finger (PPG sensor) while the reference device was placed on the upper arm as shown in Fig. 5(a). The IPG sensor was placed at different locations (A_0–C_2) to measure the signal quality in which the sensor was moved each 1 cm horizontally and each 2 cm vertically. All ipsilateral measurements were conducted in the seated position with the proposed system and reference device held over the chest area to prevent hydrostatic pressure change.

The waveforms from the proposed system have been recorded over 20 seconds at the sampling rate of 25 kHz. This sampling rate provides high resolution recordings while not overly burdening the signal processing. After recording, the received data were smoothed using a moving average filter. Thereupon, the peaks of the *dPPG/dt* waveform were detected and then the ensemble average method was performed to provide all necessary values. Finally, as given by Equation (8), those parameters have been converted to BP.

During the experiments, first, each subject was instructed to relax for 10−15 minutes. After that, the average of three pairs of sequential measurements from both the proposed and reference devices was used to obtain the calibrated parameters. As shown in Fig. 5(c), the experimental protocol includes six sessions. The first session (B1) was in the baseline period and the remaining sets alternated between handgrip exercises (E1, E2, E3) and recovery periods (R2, R3). Performing with the free right hand, handgrip maneuvers aim to acutely increase BP. Each session was conducted for 2 minutes. This study employed exercises to perturb BP because it is safe compared to cold pressor recordings and can effortlessly yield high BP variation in contrast to mental arithmetic intervention. Finally, all data points acquired from the experimental group were analyzed and evaluated.

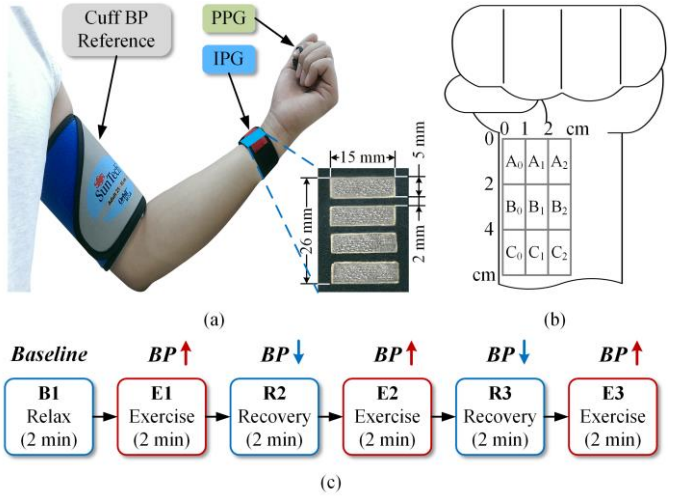

Fig. 5. The PTT-IPG-based BP model with the actual system (a), various locations of IPG sensor (b) and validation protocol (c).

III. Results

The relationships of BP, PTT and radial impedance have been established. The study computed the correlation coefficient (r) and the root-mean-squared-error (RMSE) to assess the correctness of the estimated BP values. In addition, the proposed system was further compared in terms of performance with two of the most-cited BP estimation methods in the literature.

A. Group Average Data Analysis

Fig. 6(a) shows the mean of all parameters for all subjects during validation study with the IPG sensor located at the area A_0. Due to the fact that the variabilities of those parameters in each period are greater than the changes between two adjacent stages, the standard deviation (SD) bars have been omitted for clarity. The sustained handgrip significantly increased BP level by about 20 mmHg for SBP and 15 mmHg for DBP on average. The PTT, Z_{min} (for SBP estimation), and Z_{max} (for DBP estimation) correspond well in the opposite direction of the BP variations. The mean of Z_{min} and Z_{max} decreased considerably in response to the highest SBP and DBP in E3 and E2, respectively.

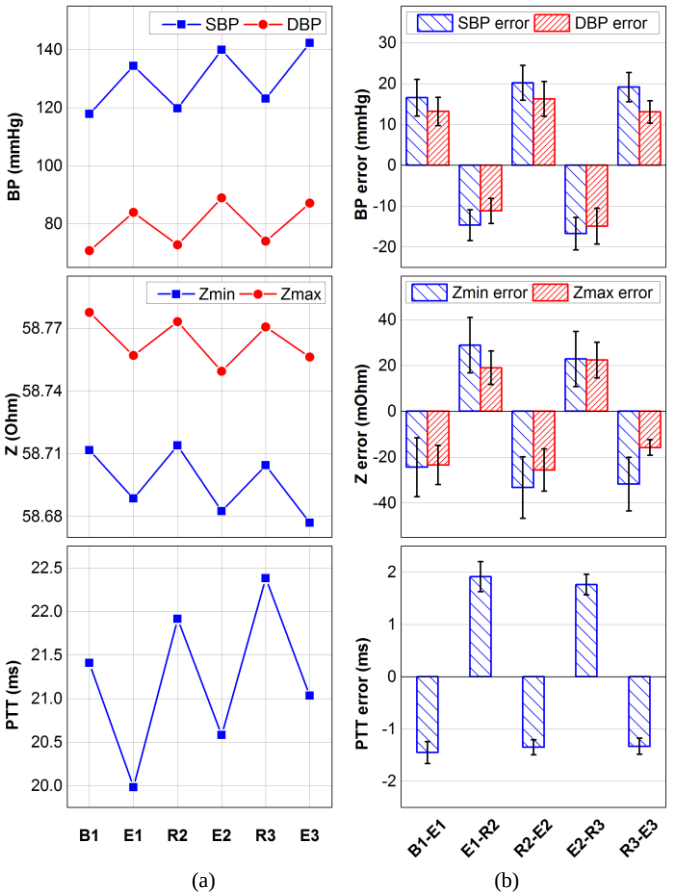

Fig. 6. Group average of SBP, DBP, Impedance Z, and PTT for each period (a) and the change of those parameters between each period (b). Error bars represent 95% CI.

This article has been accepted for publication in a future issue of this journal, but has not been fully edited. Content may change prior to final publication. Citation information: DOI 10.1109/TBME.2018.2865751, IEEE Transactions on Biomedical Engineering

However, the trend of the group average PTT seems counterintuitive. There is a tendency that PTT increased more per unit change in BP during the two recovery periods R2 and R3.

To evaluate the changing trends in detail, the mean and 95% confident interval (CI) of the difference of all group average data between each period have been analyzed in Fig. 6(b). A positive number denotes an increase, whereas a negative number denotes a decrease. Corresponding to the positive change in BP is the decline of PTT and impedance values. All the 95% CIs did not include zero, therefore, the inverse relationship between BP and those parameters was statistically significant. As shown in Fig. 6(b), all impedance values changed appropriately in response to the changes of BP in both directions. However, the magnitudes of the changes of PTT were different. When BP increased with the SBP changes from around 16.5 mmHg to 20 mmHg and the DBP changes from around 13 mmHg to 16 mmHg, PTT degraded by a similar amount of 1.45 ms, 1.35 ms, and 1.33 ms for B1-E1, R2-E2, and R3-E3 periods, respectively. In contrast, when BP decreased by about 16 mmHg for SBP and 13 mmHg for DBP on average, PTT errors in E1-R2 and E2-R3 were 32.5% and 30.5% higher than those of B1-E1 and R2-E2, respectively.

B. Performance of the Proposed Model with IPG sensor at various locations

The IPG waveforms for a representative subject at different locations are shown in Fig. 7. The high voltage at the sensing electrodes exhibits large variations in impedance and vice versa. It can be seen that the measured signal quality is better at the locations A_0, A_1, B_0, and B_1 while other locations have achieved less stable waveforms. The amount of impedance variation is lower in areas that are far away from the origin (2 cm horizontally and 4 cm vertically).

To assess the sensitivity of the IPG location, the group average correlation coefficients and RMSEs are given in Fig. 8 with the measured areas at A_0, A_1, and A_2. Those values were compared using one-way ANOVA with multiple comparisons via the Turkey test. Both estimated SBP and DBP from A_0 and A_1 achieved high correlations against the BP standard device. Those values were 0.88 ± 0.07, 0.88 ± 0.06, 0.84 ± 0.07, and 0.9 ± 0.05 for SBP and DBP of A_0 and A_1, respectively. In contrast, A_2 provided moderate correlations of 0.67 ± 0.11 (SBP) and 0.77 ± 0.1 (DBP) for estimating BP. In terms of RMSE, predicted BP levels from A_0 and A_1 yielded low errors which the difference was not significant (p-value > 0.05). Our proposed model achieved SBP RMSE of 8.47 ± 0.91 mmHg and DBP RMSE of 5.02 ± 0.73 mmHg at the area A_0 while those values were 7.66 ± 1.11 and 6.15 ± 1.3 mmHg for SBP and DBP at the area A_1, respectively. However, the proposed method showed large errors with the IPG sensor located at the area A_2 in which the RMSEs were 10.46 ± 3.27 (SBP) and 8.91 ± 3.51 (DBP) mmHg. Compared to area A_0, those values were 24% and 78% higher for estimated SPB and DBP, respectively.

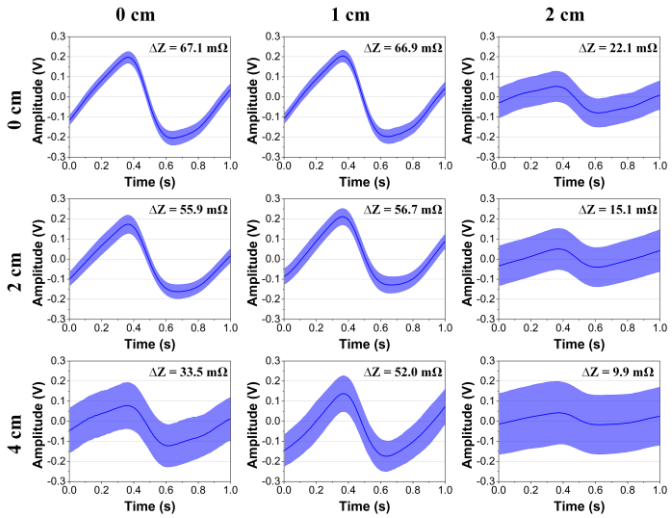

Fig. 7. The ensemble average of IPG waveforms at various locations on the forearm.

C. Performance of the Proposed Model against the most cited PTT Models

Our BP estimation was validated in comparison with two of the most cited PTT models. These models have outperformed many other PTT-base BP models and has been employed by many researchers. The first model for BP estimation is given by [33]:

$$DBP = MBP_0 + \frac{2}{\gamma}\ln\frac{PTT_0}{PTT} - \frac{PP_0}{3}\cdot\left(\frac{PTT_0}{PTT}\right)^2 \quad (12a)$$

$$SBP = DBP + PP_0\cdot\left(\frac{PTT_0}{PTT}\right)^2 \quad (12b)$$

and the second PTT model only estimates SBP through the following expression [8]:

$$SBP = SBP_0 - \frac{2}{\gamma}\frac{PTT - PTT_0}{PTT_0} \quad (13)$$

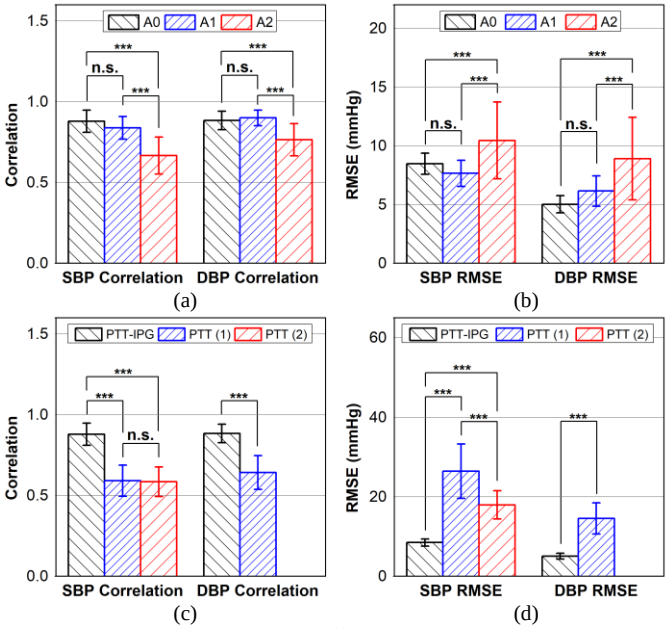

Fig. 8. Group average correlation coefficients and RMSEs between estimated SBP and DBP from our method (PTT-IPG) at various locations (a, b) and at area A_0 compared to two most-cited methods (c, d) against the reference. Triple asterisks (***) indicate statistical significance at p-value < 0.001. The symbols "n.s" indicate no significance at p-value > 0.05.

This article has been accepted for publication in a future issue of this journal, but has not been fully edited. Content may change prior to final publication. Citation information: DOI 10.1109/TBME.2018.2865751, IEEE Transactions on Biomedical Engineering

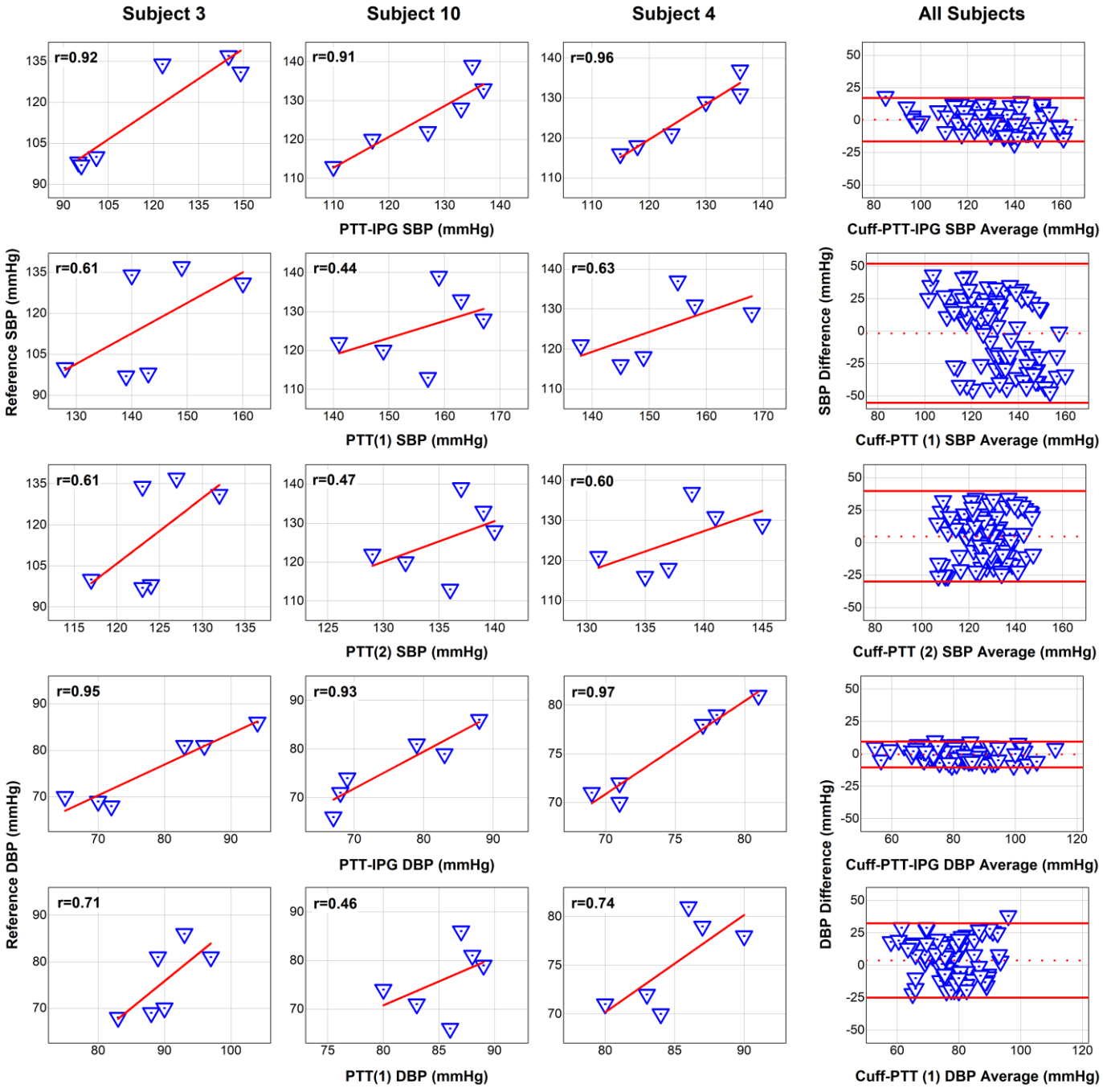

(a) (b)

Fig. 9. Representative correlation plots (a) and Bland-Altman plots for all subjects (b) of estimated SBP and DBP from proposed model (PTT-IPG), two most-cited models (PTT (1) and PTT (2)) versus reference. In (b), the dotted and solid red lines represent the mean and mean ± 1.96×SD, respectively.

in which *PP* stands for pulse pressure, γ is a subject-dependent coefficient and the parameters with the subscript "$_0$" are obtained from an initial calibration.

The area A_0 has been utilized for the validation. As shown in Fig. 8(c) and Fig. 8(d), on average, both BP levels from two most cited PTT models showed moderate correlations versus the cuff-based BP, whereas our proposed model correlated with both SBP and DBP fairly well with coefficients of 0.88 ± 0.07 and 0.88 ± 0.06, respectively. Obviously, the estimated BP values from the proposed estimation tracked better with Oscar 2 with 49% higher correlations for SBP compared to those of both two PTT models (0.59 ± 0.1 and 0.59 ± 0.09) and 38% higher correlations for DBP in comparison with those of the first model (0.64 ± 0.1). Besides that, the proposed method showed a better overall performance in terms of error. The RMSE of our method in predicting SBP was within 8.47 ± 0.91 mmHg of Oscar 2, which was 68% and 53% lower than that of the first and second PTT models, respectively. In addition, in comparison with the first PTT model, our proposed model provided a good RMSE for DBP estimation (5.02 ± 0.73 mmHg) which was 65% lower. More specifically, the first PTT model yielded SBP RMSE of 26.43 ± 6.85 mmHg and DBP RMSE of

14.53 ± 3.9 mmHg, whereas the second PTT model obtained SBP RMSE of 17.96 ± 3.54 mmHg. The improvement of our approach over the most-cited PTT models was statistically significant (p-value < 0.001), indicating a better accuracy.

The correlation plots of estimated BP from the three models against cuff BP for three representative subjects are shown in Fig. 9(a). In some circumstances, the over-response of PTT is interpreted as a result of the low correlation coefficients of BP values from two most-cited PTT models with respect to both reference SBP and DBP, whereas all BP levels from proposed PTT-IPG model did correlate well with cuff BP. The Bland-Altman plots of all predicted BP versus reference aggregated for all subjects is shown in Fig. 9(b). The bias of differences between our estimation and reference for SBP and DBP were 0.31 ± 8.55 and -0.5 ± 5.07 mmHg, respectively. The predicted DBP by our proposed model offered enhanced accuracy compared to the SBP. Furthermore, it was observed that the errors between the proposed model and cuff BP reference were smaller in comparison with those of the other methods, indicating that the predicted BP values from our model are in close agreement with those of a standard device.

IV. Discussion

This study leveraged the notion of PTT in combination with IPG measurement to enhance BP estimation. Besides demonstrating the effectiveness of using a proximal timing reference for PTT calculation, we observed that IPG method can indirectly provide information on the arterial cross-sectional area which is a good indicator of BP changes. Both IPG and PTT were utilized to estimate BP levels accordingly.

A. Effect of BP on PTT and Arterial Impedance

Earlier investigations have shown that continuous BP is composed of the oscillations at both the low frequency (LF) (around 0.1 Hz) and high frequency (HF) (between 0.2-0.3 Hz) range [34-37]. As outlined in an investigation by De Boer *et al.* [34], SBP contained HF and LF oscillations, whereas DBP obtained only LF spectrum when using intra-arterial measurement. The respiratory activity is interpreted as the main effect on the HF component in BP while the spectrum in LF range is assumed to be a result of the sympathetic vasomotor tone [36].

Our study has shown that PTT did not fully correlate well with BP. Based on the survey of HF and LF components in BP, the results of this study have verified that PTT could not reflect both two oscillators in BP. The PTT values might reflect only HF component, in other words, the change in pulse pressure. Therefore, with the inaccurately estimated DBP, the PTT-based estimated SBP is incorrect. In addition, by comparison with PTT measured in the central arteries, the respiratory activity has much less effect on that value obtained in the peripheral arteries. According to Payne *et al.* [10], due to the arterial stiffness, vascular PTT is dominated by MBP, but not SBP. Moreover, the results in prior studies could also explain that PTT may be a marker of DBP alone, or achieve DBP more accurately than SBP [10, 11, 38]. It is obvious from the previous studies and our result that PTT alone is inadequate to estimate both BP levels.

Much work has been reported on the nonlinear relationship between the diameter or the cross-section of arteries and the arterial BP [39, 40]. As we explained earlier, it is obvious that power spectrum density (PSD) of radial impedance contains a spectrum primarily influenced by heart activity since artery cross-section is continuously affected by BP [41]. Therefore, it is evident that PSD of arterial impedance is composed of both high and low variations from the BP waveform. Based on the inverse relationship between arterial impedance and BP as expressed in (3), we reasoned that Z_{min} and Z_{max} can be used to estimate beat-to-beat SBP and DBP, respectively. In addition, a number of investigations showed that the LF component of BP is caused by the SM contraction and relaxation [36, 42]. This component of arterial wall causes a change in the arterial diameter [43]. In other words, besides HF component, arterial impedance could reflect the LF variation of BP. With these considerations, we determine that the arterial impedance can be associated with the PTT to enhance BP estimation. The results have shown a significant improvement in accuracy for both estimated SBP and DBP of the additional IPG signal to PTT.

B. Locations of IPG sensor

The results showed that the area near the bracelet line has been achieved a stronger signal with higher impedance variation since the radial artery in these areas is very close to the skin surface. In other words, the measured impedance varied less in regions far from the wrist because the electric current field could not fully pass through the artery. When the IPG sensor was shifted to the right 2 cm, the signal quality was decreased because the sensor may not be located on the artery. It can be seen that the locations of IPG sensor can be varied by 1 cm horizontally and 2 cm vertically in the areas A_0, A_1, and B_0, B_1 to measure a high-quality IPG waveform.

A good signal quality provides a good reflection for impedance variation. For this reason, the proposed method estimated BP with lower RMSEs for both SBP and DBP in A_0 and A_1, whereas high errors were obtained in area A_2. The difference of correlation coefficients and RMSEs between predicting BP from area A_0 and A_1 were not statistically significant indicating that the proposed device can be adjusted in 1 cm radial direction.

C. PTT-IPG Method for BP Estimation

In this study, two sensors were located at a very short distance (around 16 cm) for the application to wearable device, therefore, the obtained PTT and error PTT are small but meaningful. Our study results showed similar PTT range with the other previous pulse transit time investigations [18-20]. While both impedance values corresponded to the changes in BP fairly well, the changes in PTT behaved differently. Bank *et al.* revealed that in low BP levels, parallel collagen fibers do not exert tension [44]. That confounding factor makes the artery cross-section changes more than the conventional regime. This was further verified in an investigation by Gao *et al.* [19]. According to the Bramwell-Hill equation, PTT depends not only on arterial compliance but also arterial cross-sectional area.

Hence, a decrease of BP, and an extra decrease in arterial cross-sectional further increases PTT. Therefore, in the two recovery periods, the changes in bias of group average PTT was larger compared to the other periods.

The other PTT models used for comparison in this work achieved low correlations and RMSEs for both BP levels in accordance with the inconsistent PTT variations. The first model showed a larger error in SBP estimation in comparison to the other models. Since SBP from that model was derived from DBP and PP, as a result, the error in predicted SBP was increased. When adding the arterial impedance parameter, the accuracy of BP measurement improved. Higher correlation coefficients are achieved for all SBP and DBP. PTT and arterial impedance tracked DBP well while SBP obtained smaller RMSEs compared to those of the other models but not as good as DBP. One way to explain this result is vascular PTT, but not PAT, is strongly inversely correlated with DBP and MBP as confirmed by Payne *et al.* [10].

PTT in this study was determined as the time delay between the points at 50% of the pulse magnitude or the peaks of the first derivative. In such cases, that PTT could reflect both BP levels. But it is worth noting that wave reflection which occurs in peripheral arteries by adding the backward wave to the forward wave increases pulse pressure. In other words, the difference between SBP and DBP becomes large with increasing distance from the heart [1]. Experimental BP waveforms show that DBP which is obtained on the BP waveform feet is less impacted by wave reflection than SBP [23]. For this reason, estimated SBP from PTT propagated from radial artery to digital artery is not sufficiently accurate with respect to the cuff SBP at the brachial artery. Another reason is that the propagated path in small arteries (e.g., from radial artery to digital artery or from femoral artery to skin vessels) are controlled by viscous blood flow. Accordingly, decreasing vessel diameter increases PTT in such arteries [45]. Another explanation for less suitable SBP RMSEs in our system is that the nonlinearity of peripheral arterial compliance could effect on the dependency of PTT and BP [7]. Moreover, the proposed estimation was performed under some assumptions. The density of blood was set as a constant for all subjects but this value varies in reality. Furthermore, the actual arterial system is not a simple tube.

As explained earlier, these considerations indicate that in addition to PTT and arterial impedance, there are still some factors that may reflect BP. However, adding arterial impedance factor would increase the accuracy of BP estimation.

D. Limitations

We further articulate on the limitations of our study. First, the recruited subjects were rather homogeneous and normotensive. The proposed model must be thoroughly assessed on a larger number human subjects. Second, the BP-varying interventions in the experimental protocol were not diverse. More specifically, we utilized three periods of the same exercise to vary BP. However, different BP perturbations must be applied to rigorously evaluate the efficacy of the proposed model. In addition, the elasticity of peripheral arteries is determined by both BP and SM contraction. Therefore, such interventions like cold pressor would provide additional value. The cold pressor test results in significant arteriolar vasoconstriction, especially peripheral arteries, thus increases the BP levels. Since the cold pressor test can provide a different physiological means of modulating BP, it is necessary for a future work to implement a cold pressor test to achieve a wide range of BP perturbation protocols. Third, regarding the standard BP reference, sphygmomanometer or invasive intra-arterial methods would constitute better gold standards than an oscillometry device. Fourth, this study did not examine day-to-day changes in the accuracy of the proposed model. The goal of this study was to assess the improvement of IPG signal in combination with PPG. For a further validation, a long-term monitoring is needed. In addition, several PTT definitions should be compared to provide the most useful indicator for estimating BP. Last but not least, besides the ensemble average method, more robust signal processing could be implemented to overcome motion artifacts and validate the system's capability for long-term monitoring.

V. Conclusion

In this paper, we demonstrate that IPG can be used as a proximal timing reference for PTT measurement and that the arterial impedance can be used in conjunction with PTT to enhance BP estimation. The PTT-IPG model was proposed and while considering the wearability of sensing modalities. The results indicated the improved performance of our method in comparison with conventional PTT-based methods on fifteen human subjects. To the best of our knowledge, this is the first study to combine PTT with the magnitude of IPG to measure BP. Our proposed model is a promising approach for BP estimation. Future efforts to overcome the noted weaknesses of the PTT-IPG method will be required including expanding the experimental protocol.

Appendix

Each term in Equation (8) is determined. The distance D is measured for each subject while the density of blood ρ is used as a constant for all subjects. Other original parameters can be obtained from a pair of measurements from the BP reference device (SBP_0, DBP_0) and the proposed device (PTT_0, Z_{max0}, Z_{min0}). The unknown constant K is given by the following equation:

$$K = \frac{\exp\left(\frac{P(t)-P_0}{\rho}\frac{PTT^2}{D^2}\right)-1}{Z_0 - Z(t)} \tag{A.1a}$$

$$= \frac{\exp\left(\frac{SBP_0 - DBP_0}{\rho}\frac{PTT_0^{\,2}}{D^2}\right)-1}{Z_{\max 0} - Z_{\min 0}} \tag{A.1b}$$

After calibration, the estimated BP can be obtained in terms of PTT and Z by comparing the change with DBP level of the calibration measurement as follow:

$$DBP = DBP_0 + \rho \frac{D^2}{PTT^2} \ln\left[1 + K\left(Z_{\max 0} - Z_{\min}\right)\right] \quad \text{(A.2a)}$$

$$SBP = DBP_0 + \rho \frac{D^2}{PTT^2} \ln\left[1 + K\left(Z_{\max 0} - Z_{\max}\right)\right] \quad \text{(A.2b)}$$

REFERENCES

[1] R. Mukkamala *et al.*, "Toward ubiquitous blood pressure monitoring via pulse transit time: theory and practice," *IEEE Trans. Biomed. Eng.,* vol. 62, no. 8, pp. 1879-1901, 2015.

[2] L. Geddes *et al.*, "Pulse transit time as an indicator of arterial blood pressure," *Psychophysiology,* vol. 18, no. 1, pp. 71-74, 1981.

[3] R. P. Smith *et al.*, "Pulse transit time: an appraisal of potential clinical applications," *Thorax,* vol. 54, no. 5, pp. 452-457, 1999.

[4] S. S. Thomas *et al.*, "BioWatch—A wrist watch based signal acquisition system for physiological signals including blood pressure," in *Proc. IEEE 36th Annu. Int. Conf. Eng. Med. Biol. Soc.*, 2014, pp. 2286-2289.

[5] S. S. Thomas *et al.*, "BioWatch: A Noninvasive Wrist-Based Blood Pressure Monitor That Incorporates Training Techniques for Posture and Subject Variability," *IEEE J. Biomed. Health Inform.,* vol. 20, no. 5, pp. 1291-1300, 2016.

[6] E. G. Lakatta, "Arterial and cardiac aging: major shareholders in cardiovascular disease enterprises," *Circulation,* vol. 107, no. 3, pp. 490-497, 2003.

[7] R. H. Cox, "Regional variation of series elasticity in canine arterial smooth muscles," *Am. J. Physiol. Heart Circ. Physiol.,* vol. 234, no. 5, pp. 542-551, 1978.

[8] W. Chen *et al.*, "Continuous estimation of systolic blood pressure using the pulse arrival time and intermittent calibration," *Med. Biol. Eng. Comput.,* vol. 38, no. 5, pp. 569-574, 2000.

[9] J. H. Shin *et al.*, "Non-constrained monitoring of systolic blood pressure on a weighing scale," *Physiol. Meas.,* vol. 30, no. 7, pp. 679, 2009.

[10] R. Payne *et al.*, "Pulse transit time measured from the ECG: an unreliable marker of beat-to-beat blood pressure," *J. Appl. Physiol.,* vol. 100, no. 1, pp. 136-141, 2006.

[11] Y. Chen *et al.*, "Continuous and noninvasive blood pressure measurement: a novel modeling methodology of the relationship between blood pressure and pulse wave velocity," *Ann. Biomed. Eng.,* vol. 37, no. 11, pp. 2222-2233, 2009.

[12] J. Sola *et al.*, "Noninvasive and nonocclusive blood pressure estimation via a chest sensor," *IEEE Trans. Biomed. Eng.,* vol. 60, no. 12, pp. 3505-3513, 2013.

[13] J. D. Lane *et al.*, "Pulse transit time and blood pressure: an intensive analysis," *Psychophysiology,* vol. 20, no. 1, pp. 45-49, 1983.

[14] C.-S. Kim *et al.*, "Ballistocardiogram as proximal timing reference for pulse transit time measurement: Potential for cuffless blood pressure monitoring," *IEEE Trans. Biomed. Eng.,* vol. 62, no. 11, pp. 2657-2664, 2015.

[15] X.-R. Ding *et al.*, "Continuous cuffless blood pressure estimation using pulse transit time and photoplethysmogram intensity ratio," *IEEE Trans. Biomed. Eng.,* vol. 63, no. 5, pp. 964-972, 2016.

[16] H. Blackburn *et al.*, "The electrocardiogram in population studies," *Circulation,* vol. 21, no. 6, pp. 1160-1175, 1960.

[17] S. L.-O. Martin *et al.*, "Weighing Scale-Based Pulse Transit Time is a Superior Marker of Blood Pressure than Conventional Pulse Arrival Time," *Sci. Rep.,* vol. 6, 2016.

[18] Y. Li *et al.*, "Noninvasive continuous blood pressure estimation with peripheral pulse transit time." pp. 66-69.

[19] M. Gao *et al.*, "Comparison of noninvasive pulse transit time estimates as markers of blood pressure using invasive pulse transit time measurements as a reference," *Physiol. Rep.,* vol. 4, no. 10, pp. e12768, 2016.

[20] X. Zhou *et al.*, "Validation of new and existing decision rules for the estimation of beat-to-beat pulse transit time," *BioMed Res. Int.,* vol. 2015, 2015.

[21] C. Holz, and E. J. Wang, "Glabella: Continuously Sensing Blood Pressure Behavior using an Unobtrusive Wearable Device," *Proceedings of the ACM on Interactive, Mobile, Wearable and Ubiquitous Technologies,* vol. 1, no. 3, pp. 58, 2017.

[22] A. M. Carek *et al.*, "SeismoWatch: Wearable Cuffless Blood Pressure Monitoring Using Pulse Transit Time," *Proceedings of the ACM on Interactive, Mobile, Wearable and Ubiquitous Technologies,* vol. 1, no. 3, pp. 40, 2017.

[23] W. Nichols *et al., McDonald's blood flow in arteries: theoretical, experimental and clinical principles*: CRC press, 2011.

[24] T. H. Huynh, and W.-y. Chung, "Radial Electrical Impedance: A Potential Indicator for Noninvasive Cuffless Blood Pressure Measurement," *J. Sensor Sci. & Tech.,* vol. 26, no. 4, pp. 239-244, 2017.

[25] D. Bergel, "The static elastic properties of the arterial wall," *J. Physiol.,* vol. 156, no. 3, pp. 445-457, 1961.

[26] J. Seo *et al.*, "Noninvasive arterial blood pressure waveform monitoring using two-element ultrasound system," *IEEE Trans. Ultrason., Ferroelect., Freq. Control,* vol. 62, no. 4, pp. 776-784, 2015.

[27] J. N. M. Kreider, and L. Hannapel, "Electrical impedance plethysmography: A physical and physiologic approach to peripheral vascular study," *Circulation,* vol. 2, no. 6, pp. 811-821, 1950.

[28] M.-C. Cho *et al.*, "A bio-impedance measurement system for portable monitoring of heart rate and pulse wave velocity using small body area." pp. 3106-3109.

[29] Y. M. Chi *et al.*, "Dry-contact and noncontact biopotential electrodes: Methodological review," *IEEE Rev. Biomed. Eng,* vol. 3, pp. 106-119, 2010.

[30] A. Pantelopoulos, and N. G. Bourbakis, "A survey on wearable sensor-based systems for health monitoring and prognosis," *IEEE Trans. Syst., Man, Cybern., Syst.,* vol. 40, no. 1, pp. 1-12, 2010.

[31] X. Ding *et al.*, "Impact of heart disease and calibration interval on accuracy of pulse transit time–based blood pressure estimation," *Physiol. Meas.,* vol. 37, no. 2, pp. 227, 2016.

[32] F. Miao *et al.*, "A Novel Continuous Blood Pressure Estimation Approach Based on Data Mining Techniques,"

IEEE J. Biomed. Health Inform., vol. 21, no. 6, pp. 1730-1740, 2017.

[33] C. Poon, and Y. Zhang, "Cuff-less and noninvasive measurements of arterial blood pressure by pulse transit time." pp. 5877-5880.

[34] R. De Boer *et al.*, "Relationships between short-term blood-pressure fluctuations and heart-rate variability in resting subjects I: a spectral analysis approach," *Med. Biol. Eng. Comput.,* vol. 23, no. 4, pp. 352-358, 1985.

[35] P. Sleight *et al.*, "Physiology and pathophysiology of heart rate and blood pressure variability in humans: is power spectral analysis largely an index of baroreflex gain?," *Clin. Sci.,* vol. 88, no. 1, pp. 103-109, 1995.

[36] A. Malliani *et al.*, "Cardiovascular neural regulation explored in the frequency domain," *Circulation,* vol. 84, no. 2, pp. 482-492, 1991.

[37] G. Baselli *et al.*, "Spectral and cross-spectral analysis of heart rate and arterial blood pressure variability signals," *Comput. Biomed. Res.,* vol. 19, no. 6, pp. 520-534, 1986.

[38] S.-y. Ye *et al.*, "Estimation of systolic and diastolic pressure using the pulse transit time," *World Acad. Sci., Eng. Technol.,* vol. 67, pp. 726-731, 2010.

[39] G. Langewouters *et al.*, "The static elastic properties of 45 human thoracic and 20 abdominal aortas in vitro and the parameters of a new model," *J. Biomech.,* vol. 17, no. 6, pp. 425-435, 1984.

[40] Y. Tardy *et al.*, "Non-invasive estimate of the mechanical properties of peripheral arteries from ultrasonic and photoplethysmographic measurements," *Clin. Phys. Physiol. Meas.,* vol. 12, no. 1, pp. 39, 1991.

[41] M. Theodor *et al.*, "Implantable impedance plethysmography," *Sensors,* vol. 14, no. 8, pp. 14858-14872, 2014.

[42] M. Pagani *et al.*, "Low and high frequency components of blood pressure variability," *Ann. N. Y. Acad. Sci.,* vol. 783, no. 1, pp. 10-23, 1996.

[43] L. H. Peterson, "Regulation of blood vessels," *Circulation,* vol. 21, no. 5, pp. 749-759, 1960.

[44] A. J. Bank *et al.*, "Contribution of collagen, elastin, and smooth muscle to in vivo human brachial artery wall stress and elastic modulus," *Circulation,* vol. 94, no. 12, pp. 3263-3270, 1996.

[45] W. R. Milnor, *Hemodynamics*: Baltimore : Williams and Wilkins, 1982.